This is a repository copy of *Tapping the Unused Potential of Photosynthesis with a Heterologous Electron Sink*.

White Rose Research Online URL for this paper:
http://eprints.whiterose.ac.uk/124121/

Version: Accepted Version

Article:
Berepiki, A., Hitchcock, A., Moore, C.M. et al. (1 more author) (2016) Tapping the Unused Potential of Photosynthesis with a Heterologous Electron Sink. ACS Synthetic Biology, 5 (12). pp. 1369-1375. ISSN 2161-5063

https://doi.org/10.1021/acssynbio.6b00100

Reuse
Unless indicated otherwise, fulltext items are protected by copyright with all rights reserved. The copyright exception in section 29 of the Copyright, Designs and Patents Act 1988 allows the making of a single copy solely for the purpose of non-commercial research or private study within the limits of fair dealing. The publisher or other rights-holder may allow further reproduction and re-use of this version - refer to the White Rose Research Online record for this item. Where records identify the publisher as the copyright holder, users can verify any specific terms of use on the publisher's website.

Takedown
If you consider content in White Rose Research Online to be in breach of UK law, please notify us by emailing eprints@whiterose.ac.uk including the URL of the record and the reason for the withdrawal request.

eprints@whiterose.ac.uk
https://eprints.whiterose.ac.uk/

Tapping the unused potential of photosynthesis with a heterologous electron sink

Adokiye Berepiki[†*], Andrew Hitchcock[‡], C. Mark Moore[†] & Thomas S. Bibby[†*]

†Ocean and Earth Sciences, National Oceanography Centre, University of Southampton, UK

‡Department of Molecular Biology and Biotechnology, University of Sheffield, UK

Abstract

Increasing the efficiency of the conversion of light energy to products by photosynthesis represents a grand challenge in biotechnology. Photosynthesis is limited by the carbon-fixing enzyme Rubisco resulting in much of the absorbed energy being wasted as heat, fluorescence or lost as excess reductant via alternative electron dissipation pathways. To harness this wasted reductant, we engineered the model cyanobacterium *Synechococcus* PCC 7002 to express the mammalian cytochrome P450 CYP1A1 to serve as an artificial electron sink for excess electrons derived from light-catalysed water-splitting. This improved photosynthetic efficiency by increasing the maximum rate of photosynthetic electron flow by 31.3%. A simple fluorescent assay for CYP1A1 activity demonstrated that the P450 was functional in the absence of its native reductase, that activity was light-dependent and scaled with irradiance. We show for the first time in live cells that photosynthetic reductant can be redirected to power a heterologous cytochrome P450. Furthermore, PCC 7002 expressing CYP1A1 degraded the herbicide atrazine, which is a widespread environmental pollutant.

Keywords: photosynthesis, P450, electron sink, photosystem, cyanobacteria, atrazine.

Photosynthesis is the pivotal biochemical reaction on the planet, providing energy for the global ecosystem. The evolution of oxygenic photosynthesis 2.7-3.2 billion years ago led to the oxygenation of the planet.[1] This subsequently hampered the efficiency of photosynthesis as oxygen competed for binding to the active site of the carbon-fixing catalyst ribulose-1, 5-bisphosphate carboxylase/oxygenase (Rubisco). As a result, the potential of photosynthesis is not achieved as the capacity for light capture and electron transport is often greater than the capacity for carbon-fixation. Photosynthetic cells therefore lose excess energy as heat and fluorescence, or through a number of alternative electron dissipation pathways.[2] Improving photosynthetic efficiency is central to efforts to increase food and/or biofuel yield, and also to realize the biotechnological potential of photosynthetic species.[3] These efforts typically focus on modification of the pigments and proteins involved in light capture, improving the efficiency/specificity of Rubisco or metabolic engineering of product formation downstream of carbon fixation.[4] However, rewiring photosynthesis such that excess reducing potential from light capture is diverted to catalyse the formation of high value products has received little attention.[5] Such a strategy can, in theory, increase the overall efficiency of photosynthetic electron usage by enabling the utilisation of electrons that would otherwise be wasted.

To increase overall photosynthetic efficiency, we installed the P450 CYP1A1 from *Rattus norvegicus* (brown rat) into *Synechococcus* PCC 7002 (henceforth *Synechococcus*) as a new electron-sink in the photosynthetic electron transport chain (Figure 1a). Cytochrome P450s are a large and diverse class of monooxygenases that split molecular oxygen (O_2), inserting one atom into the substrate and reducing the other to water (Figure 1a). CYP1A1 plays a key role in the biotransformation of drugs and other chemical compounds in mammals and has been widely studied. The catalytic activity of CYP1A1 is well-defined and easily assayed,[6] its structure has been resolved at 2.6 Å[7] and it has been expressed in other microbial hosts, allowing comparison of expression and activity levels among species.[8] We designed plasmid pSy21 to express CYP1A1 in *Synechococcus*. The expression cassette consisted of the *cyp1a1* gene, a constitutive phycocyanin promoter from

Synechocystis PCC 6803, a kanamycin resistance cassette, the *rrnB* terminator from *Escherichia coli*, and targeting flanks to guide integration to the *glpK* genomic neutral site (Figure 1b). The *cyp1a1* gene was codon-optimized for expression in *Synechococcus* and the FLAG peptide sequence was added in-frame, along with a 4 x glycine-alanine peptide linker, to the 3' of *cyp1a1* to simplify detection, quantification and purification; no other modifications were made to the *cyp1a1* sequence. This multipart construct was assembled in one step by *in vivo* recombination in *Saccharomyces cerevisiae*.[9]

Wild-type (WT) *Synechococcus* was transformed with pSy21 and, following segregation by serially sub-culturing transformants under kanamycin selection, genotyping by colony PCR confirmed that clones transformed with pSy21 were homozygous (Figure 1c). Expression of CYP1A1 was demonstrated by immunoblotting with an anti-FLAG antibody (Figure 1d) and the new strain was designated Sy21. CYP1A1 was present as a single band corresponding to its predicted molecular weight of 61 kDa. No degradation products were observed, showing that the recombinant protein was stable.

Eukaryotic P450s are generally integral membrane proteins anchored via an N-terminal transmembrane domain and require a lipid-rich environment for full activity.[10] CYP1A1 was found in the thylakoid fraction (Figure 1e), demonstrating that the native N-terminal membrane targeting domain of CYP1A1 is sufficient for localisation to the thylakoid membrane of *Synechococcus*. This feature is relevant as expression of recombinant membrane proteins in bacterial hosts is notoriously troublesome[11] and demonstrates that *Synechococcus* may be a useful production host for heterologous P450s due to the presence of internal thylakoid membranes as a platform for membrane protein expression, a strongly reducing cellular environment, and oxygenic metabolism to provide the O_2 needed for P450 catalysis.

Activity of CYP1A1 was determined by an ethoxyresorufin O-deethylation (EROD) assay, which is a rapid and sensitive means of assessing CYP1A1 activity, based on production of the fluorescent compound resorufin from ethoxyresorufin in live cells.[6] EROD demonstrated that CYP1A1 is active in *Synechococcus* (Figure 2a). CYP1A1 was active in

the absence of its native POR (P450 oxidoreductase), which suggests that reducing equivalents may have been derived from the photosynthetic machinery, potentially via ferredoxin (Figure 1a). A reductant with a midpoint redox potential similar to or more negative than NADPH (-324 mv) is required to support P450 activity. Thus the midpoint redox potential of cyanobacterial ferredoxins of between -325 and -390 mV,[12] is sufficient to reduce the P450. Indeed, it has been shown with *in vitro* experiments using chloroplasts or purified thylakoids and spinach ferredoxin that electrons derived from photosystem I (PSI) can be redirected to heterologous P450s to provide reducing equivalents in a light-dependent manner.[5, 13-17] In these *in vitro* experiments, ferredoxin serves as the electron donor instead of NADPH.

To determine the source of reducing equivalents, cells were treated with DCMU (3-(3,4-dichlorophenyl)-1,1-dimethylurea) which is a specific inhibitor of photosystem II (PSII) electron flow.[18] Treatment with 5 µM DCMU reduced resorufin production during the EROD assay by 71.4% (Figure 2b). This finding demonstrates that the majority of electrons utilized by CYP1A1 are derived via PSII-catalysed photosynthetic linear electron flow. Although DCMU prevents linear electron flow from PSII, electron transport from other pathways such as cyclic electron flow or respiration is still possible. The remaining P450 activity upon treatment with DCMU may therefore be supported by electrons from the respiratory chain which shares a b_6f complex with photosynthesis and under illumination can result in respiratory electrons being used by PSI to reduce ferredoxin.[2]

To show that P450 activity was light-dependent, cells were kept in the dark during the EROD assay. In the absence of light, resorufin production was reduced by 96.8% (Figure 2b), clearly showing that CYP1A1 activity is almost entirely light dependent in Sy21. This is further evidence for the involvement of PSI in transferring electrons to the P450, as the reduction of activity is greater in the dark than that caused by PSII inhibition alone with DCMU.

To explicitly demonstrate that CYP1A1 activity is light-driven, we determined the irradiance dependence of CYP1A1 activity by EROD *in vivo*. Cells were illuminated at

irradiances ranging from 0 to 213 µmol photons m^{-2} s^{-1}, revealing a saturating dependence of CYP1A1 activity (Figure 2c), suggesting a response that was dependent on the production of reducing equivalents from the cellular photosynthetic machinery. Although previous work has shown light-powered P450 activity using *in vitro* enzyme assays on thylakoid preparations,[5, 13-17] our finding provides the first direct evidence in live cells that photosynthetic reductant can be redirected to power a heterologous P450. Additionally, by functionally coupling an easily assayed P450 to the photosynthetic machinery we have developed a unique *in vivo* biosensor for light-generated reducing power.

Synechococcus cultures in these experiments were maintained at a light irradiance of 200 µmol photons m^{-2} s^{-1}; its optimal light irradiance is 275 µmol photons m^{-2} s^{-1} and growth rates do not increase linearly with irradiance beyond this light level.[19] However, the saturation light intensity for CYP1A1 was 29 µmol photons m^{-2} s^{-1} (Figure 2c). Thus, at physiologically relevant light irradiances P450 activity can be saturated in our expression system. This finding suggests that P450 expression does not require potentially damaging light intensities to generate measurable activity.

It has been shown previously that expression of cytochrome P450s can be used to increase resistance to herbicides.[20, 21] CYP1A1 enhances the resistance of tobacco to the potent herbicides atrazine and chloroturon and has been shown to degrade a range of polycyclic aromatic hydrocarbons demonstrating its potential for bioremediation.[20, 22] Atrazine is one of the most heavily used pesticides worldwide and is particularly problematic as an environmental pollutant because it is widespread, can persist for decades, is commonly found in drinking water and has been associated with potential endocrine and carcionogenic activity.[23] To ascertain whether expression of CYP1A1 increased resistance to atrazine, sensitivity testing was performed on solid media. Similar to other trizines, atrazine inhibits photoautotrophic growth by binding to the D1 protein in PSII and preventing reduction of plastoquinone.[18] The lethal dose of atrazine for *Synechococcus* is 1.5 µg ml^{-1}.[24] Atrazine sensitivity testing of WT *Synechococcus* and Sy21, showed that Sy21 is able to grow at atrazine concentrations of 1.5 µg ml^{-1} whereas the WT failed to produce chlorophyll and

remained unpigmented showing a cessation of photoautotrophic growth and a physiological stress response (Figure 2d). Thus, CYP1A1 enhances resistance to the herbicide atrazine. This feature can be exploited in subsequent screens to engineer both the host and the enzyme to support increased P450 activity. Importantly, this finding demonstrates that cyanobacteria can be modified for enhanced resistance to, and the ability to degrade, environmental pollutants, which, given the ubiquity and abundance of *Synechococcus* spp.,[25] is worthy of further investigation.

The fact that CYP1A1 has been expressed in other microbial systems allowed us to compare light-driven CYP1A1 activity to that powered via NAPDH and a POR in heterotrophic organisms such as *E. coli* and *S. cerevisiae* (Table 1). Light-powered CYP1A1 activity is 0.031 µmol min^{-1} g_{dcw}^{-1}, (gram dry cell weight), which is ~15 fold lower than that reported for *E. coli* but only ~5 fold lower than *S. cerevisiae*.[8] We quantified CYP1A1 in our expression system by immunoblotting using commercially available bacterial alkaline phosphatase-FLAG (BAP-FLAG) as standard (Supplementary figure 1). CYP1A1 concentration was 6.2 pmol mg^{-1} total protein (0.38 µg mg^{-1} of total protein) in strain Sy21, which is comparable to that achieved in tobacco (≤ 10 pmol mg^{-1})[21] but 33-fold less than observed in yeast microsomes (21 nmol mg^{-1} protein).[26] Therefore, it is likely that higher CYP1A1 activity could be achieved through better timing and fine-tuning of expression using strong inducible promoters.[27] Additionally, as the electron transport chain driving CYP1A1 activity competes with other electron acceptors for ferredoxin it is expected that activity will be enhanced through protein engineering to optimize the interaction between CYP1A1 and ferredoxin or by a direct fusion to ferredoxin, as has been shown recently for CYP79A1.[28] For light-powered P450-mediated biotransformations to be economically feasible a volumetric productivity of 0.001 g l^{-1} h^{-1} (equal to 0.006 µmol min^{-1} g_{dcw}^{-1}) is required for pharmaceuticals and drug metabolites.[8, 29] Thus, the activity achieved for light-driven P450 activity (0.031 µmol min^{-1} g_{dcw}^{-1}) is 5-fold more than that required. However, commercial production of fine chemicals, given their lower economic value, require much higher productivities of 0.1 g l^{-1} h^{-1} (equal to 0.6 µmol min^{-1} g_{dcw}^{-1}),[8, 29] which is 19-fold less than that

achieved for light- powered CYP1A1. Although light-driven CYP1A1 activity is less than that reported in other hosts, it is comparable and demonstrates the potential of *Synechococcus* as a production host. Indeed, a recent report has demonstrated that cyanobacteria can express multiple, active P450s.[15]

If, as we suggest, CYP1A1 is being powered by photosynthetic reductant, we might expect that activity of the P450 would function as an artificial electron sink, increasing the light saturation level of photosynthesis and associated optimal irradiance levels. Physiological parameters were assessed using Fast Repetition Rate fluorometry[30] (FRRf) to determine the effects of CYP1A1 on the characteristics of the photosynthetic electron transport chain. The chlorophyll *a* content and functional absorption cross sections of PSII (σ_{PSII}) were similar in the WT and Sy21 (Table 2) consistent with CYP1A1 expression having minimal direct impact on photosynthetic organisation. The apparent photosynthetic energy conversion efficiency (F_v/F_m) is slightly elevated in Sy21 suggesting it is using light energy more effectivity, however this does not result in an increase in growth rate which remains similar to WT (Figure 3a). Moreover, the maintained growth rates suggest that P450 activity does not significantly deplete the cell of reducing equivalents required for growth and maintenance. Importantly, Sy21 had a 31.3% higher maximum PSII electron transport rate (ETR_{max}; Table 2 and Figure 3b) and correspondingly a 38.2% higher light saturation intensity (E_k) than the WT, demonstrating the increased capacity of Sy21 to process photosynthetically derived electrons. This finding also demonstrates that the expressed P450 can reduce endogenous substrates, which is unsurprising given the range of compounds CYP1A1 is able to act upon.[7, 22] Moreover, treatment of cells with 10 µM of the P450 inhibitor α-naphthoflavone,[31] which completely abrogated CYP1A1 activity in strain Sy21 (Supplementary Figure 2), reduced both ETR_{max} and E_k to WT levels in Sy21, while having minimal effect on the WT (Figure 3b). Thus, rather than competing with the photosynthetic dark reactions for reductant and hence potentially suppressing overall growth rates, the expression and activity of CYP1A1 acts as a significant additional sink for electrons downstream of PSII. Enhanced linear photosynthetic electron transport was thus

maintained at saturating light intensities by the re-direction of excess electrons to CYP1A1. As light-powered P450 activity is concomitant with the irreversible hydroxylation of a substrate it is therefore distinct from native dissipative electron sinks such as water-water cycles catalysed by Flv1/3 enzymes.[32] The increase in maximum electron flux in Sy21 raises the possibility that light-powered P450 activity will contribute to enhanced proton motive force and ATP generation, however, this possibility requires further experimental validation.

In summary, we have expressed a mammalian P450 in a cyanobacterial host and demonstrated with a simple fluorescent assay in live cells that its activity was light-dependent and scaled with irradiance. The P450 is active in the absence of its native reductase, is dependent on electrons derived from photosynthesis and confers resistance to the herbicide atrazine. Hence, this paper describes how a widespread and important aquatic microbe may be genetically engineered for the light-driven bioremediation of environmental pollutants. Importantly, expression of CYP1A1 increased the optimal level of irradiance for photosynthetic electron transport meaning that at supra-optimal irradiances electrons that would otherwise be wasted are now redirected to power product formation by a heterologous enzyme. Therefore, we have re-engineered photosynthesis such that new products can be formed independently of the inherent catalytic limitations of Rubisco. This study represents the first demonstration of a highly-promising strategy to improve the overall efficiency of electron use during photosynthesis at supersaturating irradiances for the production of clean and sustainable biomolecules and should be applicable to any photosynthetic species.

Methods

Chemicals. Water was from a Milli-Q filtration system (Millipore). Chemicals used in this study were purchased from Sigma, Invitrogen or Fisher. Antibiotics were purchased from Sigma or Melford Biolabs. Plasmid DNA was purified with mini-prep kits from Zymo Research. Q5 polymerase was purchased from New England Biolabs and was used for all PCRs with the exception of colony PCRs which were carried out using Phire Green Hot Start II polymerase from Thermo Scientific. FastDigest restriction enzymes were purchased from Thermo Scientific.

Culture conditions. *Escherichia coli* strain XL1 blue was used for cloning purposes and plasmid maintenance and was grown in LB containing the appropriate antibiotic (kanamycin 50 µg ml^{-1}). For *in vivo* recombination the *S. cerevisiae* strain FY834 was used and grown in YPD or SC-uracil.

WT *Synechococcus* PCC 7002 was obtained from the National Center for Marine Algae and Microbiota (Bigelow Laboratory for Ocean Sciences, Maine). WT and engineered strains of *Synechococcus* were grown in A^+ medium containing sodium nitrate (1 g l^{-1}) supplemented with kanamycin at 100 µg ml^{-1} where appropriate. Solid A^+ media was made with 1% bacto-agar and 1 mM sodium thiosulfate. For expression studies and analysis of growth rates, strains were grown in 40 ml of liquid medium in 250 ml baffled flasks; cultivation was under continuous white LED illumination at 200 µmol photons m^{-2} s^{-1} at 37 ºC with shaking at 200 rpm in an algaetron growth chamber (PSI Instruments). To determine growth rates, $OD_{730\ nm}$ was measured every 24 h for 6 days with a spectrophotometer (model 7315, Jenway). These conditions are referred to as standard growth conditions. Illumination irradiance was monitored with a Li-Cor Li-250A light sensor equipped with a LI-190SA quantum sensor. Transformation plates and atrazine-supplemented plates were incubated in

247 a multitron growth chamber (Infors AG) with continuous cool white fluorescent illumination at
248 50-70 µmol photons m^{-2} s^{-1} at 30 ºC.
249
250 **Ethoxyresorufin O-deethylation (EROD) assay for CYP1A1 activity.** CYP1A1 activity
251 was measured using an EROD assay.[6] Cells from an exponentially growing culture were
252 adjusted to $OD_{730\ nm}$ 1.0 with A^+ medium and 100 µl of the suspension was dispensed in
253 triplicate to a black 96-well microplate (Grenier Bio-One) and allowed to equilibrate for 10
254 min under standard growth conditions. EROD was started by the addition of 100 µl of 5 µM
255 7-ethoxyresorufin in A^+ medium to a final concentration of 2.5 µM. The formation of the
256 fluorescent product resorufin was measured in a microplate reader (excitation 544 nm,
257 emission 590 nm; Fluostar Optima by BMG Labtech). For inhibitor studies, DCMU was
258 dissolved in ethanol and used at 5 µM and the CYP1A1 inhibitor α-naphthoflavone was
259 dissolved in DMSO and used at 10 µM. Inhibitors were added to cells at the same point as
260 7-ethoxyresorufin.
261 The effect of DCMU and light irradiance on CYP1A1 activity was determined using
262 the EROD assay with the following modifications. Cells were prepared and dispensed into a
263 microplate as describe above, covered in foil to exclude light then incubated in standard
264 conditions for 1 h. This step serves to oxidize the electron transport chain and deplete
265 cellular reducing equivalents. The assay was commenced by the addition of EROD as
266 described above and where appropriate the light intensity was varied using layers of neutral
267 density paper overlaid on the appropriate wells to yield a range of irradiance from 16-213
268 µmol photons m^{-2} s^{-1}. Samples to remain in the dark were covered with foil. Exposure of the
269 samples to light was minimized throughout the experiment and resorufin production was
270 measured as described above.
271 To convert fluorescent units from the plate reader to resorufin formation, a standard
272 curve was generated using commercially available resorufin (Sigma). Specific activity was
273 determined by calculating the rate of product formation between two time intervals - 30 and

60 min - where the rate of product formation was constant. Activity is given as µmol resorufin min^{-1} g_{dcw}^{-1}.

Biophysical measurements. Samples from exponentially growing cultures ($OD_{730\ nm}$ 0.6-0.7) were measured on a FastOcean sensor integrated with a Act2 Laboratory system (Chelsea Technologies Group Ltd.) using the FRRf technique.[30] All samples were dark acclimated for 30 min prior to analysis. Fluorescence transients were measured through excitation by 450 nm and 624 nm LEDs to excite both chlorophyll *a* and phycocyanin simultaneously using a saturating sequence of 100 1 µs flashlets at a 2 µs repetition rate. Measurements of fluorescence parameters over an imposed actinic light gradient (Fluorescence Light Curves, FLCs), were subsequently used to determine light response of photosynthetic electron transport.[33] The FLC consisted of 16 steps, ranging from 0-1600 µmol photons m^{-2} s^{-1}. Fluorescence transients were fitted to a model[30] using the Act2 software to determine the maximum quantum yield for PSII as the ratio of variable to maximal fluorescence (F_v/F_m) and the functional absorption cross section serving PSII photochemistry (σ_{PSII}) in the dark, alongside the absolute electron transport rate (ETR) through PSII:

$$ETR = \sigma_{PSII}\,(F_q'/F_m') \,/\, (F_v/F_m)$$

where F_q'/F_m' is the ratio of variable to maximal fluorescence measured under actinic light. The light response of ETR was subsequently fitted to a standard model to derive the maximum PSII electron transport rate (ETR_{max}) and the light saturation parameter (E_k).

Molecular cloning, Immunoblotting and quantification of CYP1A1, Thylakoid preparation, Dry cell weight determination, Chlorophyll-*a* measurement. See Supporting Information for details.

Tables

Table 1. Comparison of maximum specific ethoxyresorufin O-deethylation activities (µmol min^{-1} g_{dcw}^{-1}) in different recombinant microorganisms expressing CYP1A1.

Host	**µmol min^{-1} g_{dcw}^{-1}**	**Ref.**
Synechococcus	0.031	this study
E. coli	0.43	8
S. cerevisiae	0.16	8

Table 2. Comparison of chlorophyll *a* content, F_v/F_m, $\sigma_{PSII,}$ and electron transport rate in the WT and Sy21.

Strain	**chlorophyll *a* (µg ml^{-1} $OD_{730\ nm}^{-1}$)**	**photosynthetic energy conversion efficiency (F_v/F_m)**	**PSII functional absorption cross section (σ_{PSII})**	**Maximum electron transport rate (e^- $RCII^{-1}$ s^{-1})**
WT	4.90 ± 0.17	0.414 ± 0.002	2.50 ± 0.05	356.6
Sy21	4.84 ± 0.26	0.436 ± 0.011	2.48 ± 0.03	468.3

Associated content

Supporting information

Primers for PCR are presented in Supplementary Table 1; Quantification of CYP1A1 and CYP1A1 inhibitor analysis are shown in Supplementary Figure 1 and 2, respectively. Methods for molecular cloning, immunoblotting and quantification of CYP1A1, thylakoid preparation, dry cell weight determination, and chlorophyll-*a* measurement are supplied as Supporting Information.

Additional information

Corresponding Authors

*(A.B.) Tel.: +44 (0) 2380 599 346. E-mail: a.berepiki@soton.ac.uk

*(T.S.B.) Tel.: +44 (0) 2380 596 446. E-mail: tsb@noc.soton.ac.uk

Author contributions

A.B. conceived the project. A.B. and T.S.B. designed the experiments. A.B. performed most of the experiments. A.H. determined the localisation of CYP1A1. A.B., A. H., C.M.M. and T.S.B. analysed and interpreted the data. A.B. and T.S.B. wrote the paper and all authors edited the manuscript.

Notes

The authors declare no competing financial interests.

Acknowledgements

This research was funded by a BBSRC grant (www.bbsrc.ac.uk) to T.S.B. (BB/M011305/1). The authors wish to thank Nicola Pratt for help with chlorophyll measurements and Jane Saunders for critical reading of the manuscript.

Figure legends

Figure 1. Expression and localisation of CYP1A1 in *Synechococcus*. (a) Diagram of an artificial electron transport chain that uses light to power a heterologous P450. Photosynthetic electrons derived from water splitting at photosystem II (PSII; not shown) are used by photosystem I (PSI) to reduce ferredoxin (Fd), which potentially serves as the electron donor for the P450. (b) Diagram showing the CYP1A1 expression cassette and the genomic neutral site for integration. (c) Colony PCR on WT and transformed (c1-4) *Synechococcus* colonies using primer pair NS1 seg fw and NS1 seg rv. The band sizes correlate with the expected sizes of 4048 bp for transformants and 397 bp for the WT. (d) Immunoblot with anti-FLAG antibody on 30 µg of total protein from WT and strain Sy21. CYP1A1 was detected at the predicted mass of 61 kDa as indicated by the arrow. The lower panel is SYPRO ruby staining of a duplicate protein gel showing equal loading of each lane. (e) Immunoblot with anti-FLAG antibody on thylakoids extracted from the WT and Sy21. For each sample 30 µg protein was loaded. The arrow indicates CYP1A1.

Figure 2. CYP1A1 activity depends on reducing equivalents from photosystem II (PSII), is proportional to light irradiance and enhances resistance to atrazine. CYP1A1 activity was measured via an ethoxyresorufin O-deethylation (EROD) assay in live cells using a microplate reader. CYP1A1 catalyses the formation of the fluorescent product resorufin from the non-fluorescent substrate ethoxyresorufin. Measurements were made on three biological replicates 1 h after the addition of 5 µM ethoxyresorufin. Each experiment was repeated a minimum of three times and results from a typical experiment are shown. Error bars represent the standard error of triplicate measurements. Statistical significances were inferred by the Student's *t* test; $***P < 0.001$. (a) CYP1A1 activity in WT and Sy21. (b) CYP1A1 activity in the absence of PSII activity or light. Cells were dark adapted for 1 h to deplete reducing equivalents then treated with the PSII inhibitor DCMU (3-(3,4-

368 dichlorophenyl)-1,1-dimethylurea) or kept in the dark. (c) CYP1A1 activity at different light
369 irradiances. Cells were dark adapted for 1 h to deplete reducing equivalents then illuminated
370 at different irradiances. Standard curve analysis showed the saturating irradiance for
371 CYP1A1 activity was 29 µmol photons m^{-2} s^{-1}. (d) Expression of CYP1A1 increases
372 resistance to the herbicide atrazine (atz). Sensitivity was assessed by spot testing on solid
373 media containing 0, 0.5, 1 or 1.5 µg ml^{-1} atz. Plates were incubated at 30 ºC for 7 days with
374 illumination at 200 µmol photons m^{-2} s^{-1}. The cell number for the spots in each panel are,
375 from left to right, 2 x 10^5, 1 x 10^4 and 5 x 10^2.
376
377 **Figure 3.** Expression of CYP1A1 increases the optimal irradiance for photosynthesis. Data
378 are the average of three independent experiments. Error bars represent the standard error of
379 triplicate measurements. (a) Comparison of growth rate of WT to Sy21. (b) The absolute
380 electron transport rate from the reaction center of photosystem II (e^- $RCII^{-1}$ s^{-1}) for WT and
381 Sy21 at different irradiances assessed via Fast Repetition Rate fluorometry (FRRf). Cells
382 were treated with 10 µM of the CYP1A1 inhibitor α-naphthoflavone or the diluent control
383 DMSO.
384
385
386

References

[1] Falkowski, P. G., and Isozaki, Y. (2008) The Story of O_2, *Science 322*, 540-542.

[2] Lea-Smith, D. J., Bombelli, P., Vasudevan, R., and Howe, C. J. (2016) Photosynthetic, respiratory and extracellular electron transport pathways in cyanobacteria, *Biochim. Biophys. Acta 1857*, 247-255.

[3] Stephenson, P. G., Moore, C. M., Terry, M. J., Zubkov, M. V., and Bibby, T. S. (2011) Improving photosynthesis for algal biofuels: toward a green revolution, *Trends Biotechnol. 29*, 615-623.

[4] Cotton, C. A. R., Douglass, J. S., De Causmaecker, S., Brinkert, K., Cardona, T., Fantuzzi, A., Rutherford, A. W., and Murray, J. W. (2015) Photosynthetic constraints on fuel from microbes, *Front. Bioeng. Biotechnol. 3*.

[5] Nielsen, A. Z., Ziersen, B., Jensen, K., Lassen, L. M., Olsen, C. E., Moller, B. L., and Jensen, P. E. (2013) Redirecting photosynthetic reducing power toward bioactive natural product synthesis, *ACS Synth. Biol. 2*, 308-315.

[6] Mohammadi-Bardbori, A. (2014) Assay for quantitative determination of CYP1A1 enzyme activity using 7-Ethoxyresorufin as standard substrate (EROD assay), *Protoc. Exch.*, doi:10.1038/protex.2014.1043.

[7] Walsh, A. A., Szklarz, G. D., and Scott, E. E. (2013) Human cytochrome P450 1A1 structure and utility in understanding drug and xenobiotic metabolism, *J. Biol. Chem. 288*, 12932-12943.

[8] Cornelissen, S., Julsing, M. K., Schmid, A., and Buhler, B. (2012) Comparison of microbial hosts and expression systems for mammalian CYP1A1 catalysis, *J. Ind. Microbiol. Biotechnol. 39*, 275-287.

[9] Oldenburg, K. R., Vo, K. T., Michaelis, S., and Paddon, C. (1997) Recombination-mediated PCR-directed plasmid construction *in vivo* in yeast, *Nucleic Acids Res. 25*, 451-452.

[10] Munro, A. W., Girvan, H. M., Mason, A. E., Dunford, A. J., and McLean, K. J. (2013) What makes a P450 tick?, *Trends Biochem. Sci. 38*, 140-150.

[11] Zelasko, S., Palaria, A., and Das, A. (2013) Optimizations to achieve high-level expression of cytochrome P450 proteins using Escherichia coli expression systems, *Protein. Expr. Purif. 92*, 77-87.

[12] Cammack, R., Rao, K. K., Bargeron, C. P., Hutson, K. G., Andrew, P. W., and Rogers, L. J. (1977) Midpoint redox potentials of plant and algal ferredoxins, *Biochem. J. 168*, 205-209.

[13] Lassen, L. M., Nielsen, A. Z., Olsen, C. E., Bialek, W., Jensen, K., Moller, B. L., and Jensen, P. E. (2014) Anchoring a plant cytochrome P450 via PsaM to the thylakoids in *Synechococcus* sp. PCC 7002: evidence for light-driven biosynthesis, *PLoS ONE 9*, e102184.

[14] Gangl, D., Zedler, J. A., Wlodarczyk, A., Jensen, P. E., Purton, S., and Robinson, C. (2015) Expression and membrane-targeting of an active plant cytochrome P450 in the chloroplast of the green alga *Chlamydomonas reinhardtii*, *Phytochemistry 110*, 22-28.

[15] Wlodarczyk, A., Gnanasekaran, T., Nielsen, A. Z., Zulu, N. N., Mellor, S. B., Luckner, M., Thofner, J. F., Olsen, C. E., Mottawie, M. S., Burow, M., Pribil, M., Feussner, I., Moller, B. L., and Jensen, P. E. (2015) Metabolic engineering of light-driven cytochrome P450 dependent pathways into *Synechocystis* sp. PCC 6803, *Metab. Eng. 33*, 1-11.

[16] Kim, Y.-S., Hara, M., Ikebukuro, K., Miyake, J., Ohkawa, H., and Karube, I. (1996) Photo-induced activation of cytochrome P450/reductase fusion enzyme coupled with spinach chloroplasts, *Biotechnol Tech 10*, 717-720.

[17] Gnanasekaran, T., Karcher, D., Nielsen, A. Z., Martens, H. J., Ruf, S., Kroop, X., Olsen, C. E., Motawie, M. S., Pribil, M., Moller, B. L., Bock, R., and Jensen, P. E. (2016) Transfer of the cytochrome P450-dependent dhurrin pathway from Sorghum bicolor into Nicotiana tabacum chloroplasts for light-driven synthesis, *J Exp Bot 67*, 2495-2506.

[18] Trebst, A. (1980) Inhibitors in electron flow: Tools for the functional and structural localization of carriers and energy conservation sites, In *Methods Enzymol.* (Anthony San, P., Ed.), pp 675-715, Academic Press.

[19] Bernstein, H. C., Konopka, A., Melnicki, M. R., Hill, E. A., Kucek, L. A., Zhang, S., Shen, G., Bryant, D. A., and Beliaev, A. S. (2014) Effect of mono- and dichromatic light quality on growth rates and photosynthetic performance of *Synechococcus* sp. PCC 7002, *Front. Microbiol. 5*, 488.

[20] Ohkawa, H., Imaishi, H., Shiota, N., Yamada, T., Inui, H., and Ohkawa, Y. (1998) Molecular mechanisms of herbicide resistance with special emphasis on cytochrome P450 monooxygenases, *Plant Biotechnol. 15*, 173-176.

[21] Shiota, N., Nagasawa, A., Sakaki, T., Yabusaki, Y., and Ohkawa, H. (1994) Herbicide-resistant tobacco plants expressing the fused enzyme between rat cytochrome P4501A1 (CYP1A1) and yeast NADPH-cytochrome P450 oxidoreductase, *Plant Physiol. 106*, 17-23.

[22] Sakaki, T., Yamamoto, K., and Ikushiro, S. (2013) Possibility of application of cytochrome P450 to bioremediation of dioxins, *Biotechnol. Appl. Biochem. 60*, 65-70.

[23] Jablonowski, N. D., Schaffer, A., and Burauel, P. (2011) Still present after all these years: persistence plus potential toxicity raise questions about the use of atrazine, *Environ. Sci. Pollut. Res. Int. 18*, 328-331.

[24] Buzby, J. S., Mumma, R. O., Bryant, D. A., Gingrich, J., Hamilton, R. H., Porter, R. D., Mullin, C. A., and Stevens, S. E., Jr. (1987) Genes with mutations causing herbicide resistance from the cyanobacterium *Synechococcus* PCC 7002, In *Progress in Photosynthesis Research* (Biggins, J., Ed.), pp 757-760, Springer Netherlands.

[25] Waterbury, J. B., Watson, S. W., Guillard, R. R. L., and Brand, L. E. (1979) Widespread occurrence of a unicellular, marine, planktonic, cyanobacterium, *Nature 277*, 293-294.

[26] Sakaki, T., Kominami, S., Takemori, S., Ohkawa, H., Akiyoshi-Shibata, M., and Yabusaki, Y. (1994) Kinetic studies on a genetically engineered fused enzyme between rat cytochrome P450 1A1 and yeast NADPH-P450 reductase, *Biochemistry 33*, 4933-4939.

[27] Markley, A. L., Begemann, M. B., Clarke, R. E., Gordon, G. C., and Pfleger, B. F. (2015) Synthetic biology toolbox for controlling gene expression in the cyanobacterium *Synechococcus* sp. strain PCC 7002, *ACS Synth. Biol. 4*, 595-603.

[28] Mellor, S. B., Nielsen, A. Z., Burow, M., Motawia, M. S., Jakubauskas, D., Moller, B. L., and Jensen, P. E. (2016) Fusion of Ferredoxin and Cytochrome P450 Enables Direct Light-Driven Biosynthesis, *ACS Chem Biol 11*, 1862-1869.

[29] Julsing, M. K., Cornelissen, S., Buhler, B., and Schmid, A. (2008) Heme-iron oxygenases: powerful industrial biocatalysts?, *Curr Opin Chem Biol 12*, 177-186.

[30] Kolber, Z. S., Prášil, O., and Falkowski, P. G. (1998) Measurements of variable chlorophyll fluorescence using fast repetition rate techniques: defining methodology and experimental protocols, *Biochim. Biophys. Acta 1367*, 88-106.

[31] Shimada, T., Yamazaki, H., Foroozesh, M., Hopkins, N. E., Alworth, W. L., and Guengerich, F. P. (1998) Selectivity of polycyclic inhibitors for human cytochrome P450s 1A1, 1A2, and 1B1, *Chem. Res. Toxicol. 11*, 1048-1056.

[32] Allahverdiyeva, Y., Mustila, H., Ermakova, M., Bersanini, L., Richaud, P., Ajlani, G., Battchikova, N., Cournac, L., and Aro, E. M. (2013) Flavodiiron proteins Flv1 and Flv3 enable cyanobacterial growth and photosynthesis under fluctuating light, *Proceedings of the National Academy of Sciences of the United States of America 110*, 4111-4116.

[33] Suggett, D. J., Moore, C. M., and Geider, R. J. (2010) Estimating aquatic productivity from active fluorescence measurements, In *Chlorophyll a Fluorescence in Aquatic Sciences: Methods and Applications* (Suggett, J. D., Prášil, O., and Borowitzka, A. M., Eds.), pp 103-127, Springer Netherlands, Dordrecht.

Supporting Information

Supplementary Table 1. Primers used to construct the CYP1A1 expression vector and for genotyping analysis.

Primer name	nucleotide sequence 5'-3'
NS1 LF fw LL ext	ACGCGCCCTGACGGGCTTGTCTGCTCGTTTAAACtgaagcgattggctatgatctacc
NS1 LF rv	TTCTATCGCCTTCTTGACGAGTTCTTCTGAAGATCTttttgatgggccatggtcat
Kan fw	tcagaagaactcgtcaagaaggcg
Kan rv	tggacagcaagcgaaccgga
Pcpcb fw kan ext	CAATTCCGGTTCGCTTGCTGTCCAAGATCTgttataaaataaacttaacaaatctatacc
Pcpcb rv 6H ext	TGCGGCCGCATGGTGATGGTGATGATGCATtgaattaatctcctacttgactttatg
TrrnB fw Pcpcb ext	ACTCATAAAGTCAAGTAGGAGATTAATTCAatgcatcatcaccatcaccatgc
TrrnB rv NS1 RF ext	ACGATTACCAGTGGTACCGAGGTCTAACGCcctaggagcggatacatatttgaatg
NS1 RF fw TrrnB ext	AATACATTCAAATATGTATCCGCTCCTAGGgcgttagacctcggtaccac
NS1 RF rv RR ext	GAAGATCCTTTGATCTTTTCTACGGGGTTTAAACgctcgactgcaccgttgg
NS1 seg fw	tttggatcgttggcagttgg
NS1 seg rv	tgttgacgacctgttgcatg

Bases that serve as extensions to guide recombination and are not complementary are shown in uppercase.

Molecular cloning. All primers used in this study are listed in Supplementary Table 1 and PCRs were run using the manufacturers cycling conditions. WT *Synechococcus* genomic DNA was used as a template to amplify genomic sequences.

Expression cassettes for *Synechococcus* were generated by *in vivo* recombination in yeast and were designed to integrate into the *glpK* pseudogene (SYNPCC7002_A2842). All DNA fragments used were generated by PCR or from synthetic DNA. To generate targeting flanks, two ~0.5 kb regions were amplified from *glpK* using primer pair NS1 LF fw LL ext and NS1 LF rv for the left flank and primer pair NS1 RF fw TrrnB ext and NS1 RF rv RR ext for the right flank. The kanamycin selection marker was amplified from pGFP::hph::loxP with primer pair kan fw and kan rv. The *cpcBA* promoter was amplified from WT *Synechocystis* PCC 6803 using the primer pair Pcpcb fw kan ext and Pcpcb rv 6H ext. The *E. coli rrnB*

terminator was amplified from pDF-lac with primer pair TrrnB fw Pcpcb ext and TrrnB rv NS1 RF ext. The *cyp1a1* gene (NCBI reference: NM_012540.2) from *R. norvegicus* was modified to include the FLAG epitope at the C-terminus, codon-optimized for expression in *Synechococcus* and synthesized by GeneArt (Thermo Scientific). The *cyp1a1* gene and *FLAG* sequence are fused by a 4 x glycine-alanine linker. The pKU acceptor vector, into which the DNA fragments were recombined, was linearized by PCR with primer pair pKU LL rv and pKU RR fw. The amplicons generated have 30 bp extensions at the 5' and 3'-end that permit recombination with the adjacent amplicon. Amplicons consisting of targeting flanks, a selection marker, promoter, *CYP1A1* and terminator were co-transformed into yeast, along with the linearized acceptor vector pKU, for assembly via its endogenous recombination system.[9] Yeast transformations were carried out with the lithium acetate/PEG method and grown in 20 ml of SC-uracil for selection. The assembled plasmid was transferred from yeast to *E. coli* and following restriction digest screening and confirmation of the correct vectors by DNA sequencing, the cassette was released from the backbone by digestion with *Pme*I and transformed into *Synechococcus* by adding the DNA (~ 1 µg) to 3 ml of cells in exponential growth phase ($OD_{730\ nm}$ 0.6-0.7). After 16-18 h under standard growth conditions cell were plated out. Single colonies from transformation plates were serially sub-cultured in liquid medium under standard growth conditions to obtain fully segregated strains. Integration and segregation was confirmed by colony PCR using primers NS1 seg fw and NS1 seg rv. Two independent transformants, Sy21a and Sy21b, were selected and cryopreserved. No differences in CYP1A1 expression were observed between these transformants (data not shown). All experiments were carried out on Sy21a, which was renamed as Sy21.

Immunoblotting and quantification of CYP1A1. Whole cell extracts of *Synechococcus* strains were prepared from 40 ml cultures. Cells were harvested by centrifugation at 3,500 *g* for 10 min at room temperature (RT; 21 °C). Approximately 100 mg of 0.1 mm zirconia beads (Biospec Products) was added to the pellet followed by the addition of an equal volume (~ 300 µl) of SDS lysis buffer (200 mM NaCl, 25 mM EDTA, 0.5% (w/v) SDS, 200

47 mM Tris-Cl, pH 8.5). The cells were lysed in a Tissue lyser (Qiagen) for 2 x 30 s cycles at a
48 frequency of 30 Hz. The tubes were then heated to 95 °C in a heat block for 10 min, cooled
49 briefly on ice then cell debris was pelleted by centrifugation at 17,000 *g* for 10 min at 4 °C.
50 The cleared lysate was removed and quantified for total protein using a bicinchoninic acid
51 (BCA) protein assay (Pierce) with bovine serum albumin (BSA) as the standard. We used
52 BAP conjugated to the FLAG peptide at the C-terminus (BAP-FLAG) as a standard for
53 quantitative immunoblots. BAP-FLAG was quantified in the same manner as whole cell
54 extracts and then diluted in a 1 mg ml^{-1} solution of BSA, which minimizes nonspecific binding
55 of the protein standard to plasticware. Protein samples were prepared in LDS loading buffer
56 (Invitrogen) containing DTT at 50 mM and heated for 10 min at 70 °C. Thirty micrograms of
57 total protein was separated by electrophoresis on a 4-12% gradient Bis-tris NuPAGE gel in
58 MES buffer (Invitrogen) in a Novex XCell SureLock Mini Cell (Invitrogen) for 35 min at 200 V.
59 Where appropriate, BAP-FLAG standard was loaded in amounts ranging from 2-10 ng. Gels
60 were then stained for total protein using SYPRO Ruby (Invitrogen), according to the
61 manufacturer's instructions, or used for immunoblots.
62 For immunoblotting, gels were transferred to an Millipore Immobilon-P 0.45 µm
63 polyvinyl fluoride (PVDF) membrane in NuPAGE transfer buffer (Invitrogen) for 60 min at 30
64 V in a XCell blot module (Invitrogen) and the membrane was then incubated in blocking
65 solution (TBS-T; 20 mM Tris-Cl, 150 mM NaCl, 0.02% (v/v) Tween-20, pH 7.6 supplemented
66 with 2% (w/v) ECL Advance blocking reagent; GE Healthcare) for 1 h. All incubation steps
67 were carried out on a rocker table. Blocking agent was discarded and the membrane was
68 incubated with mouse monoclonal anti-FLAG M2-peroxidase (HRP) antibody (Sigma; diluted
69 to 1:1,000 in blocking solution). Membranes were washed for 3 x 5 min in TBS-T then
70 incubated for 5 min in ECL substrate consisting of 0.5 ml each of SuperSignal West Dura
71 reagent A and B (Thermo Scientific) and imaged using a Versa-Doc Imaging system
72 (BioRad). For quantitative immunoblots, images were analysed using Image Lab 3.0
73 software (BioRad) for quantification of proteins.
74

Thylakoid membrane preparation. To prepare membranes enriched in thylakoids, cells from 40 ml cultures were harvested by centrifugation as described above and the pellet was re-suspended in 25 mM potassium phosphate buffer pH 7.4 with 100 mM NaCl and 10 mM $MgCl_2$. An equal volume of 0.1 mm zirconium beads was added and the cells were subjected to 8 pulses of bead beating for 20 s in a Mini-beadbeater-16 (Biospec Products), with 2 min intervals of incubation on ice between the pulses. The liquid fraction was centrifuged for 1 min at 2000 *g* at RT to remove contaminating beads and the cell lysate was loaded onto a step sucrose gradient made from solutions of 30 % (w/v) and of 50 % (w/v) sucrose. The gradient was made in a SW41 centrifuge tube and the cell lysate was loaded on top of the gradient and then centrifuged at 154,000 *g* in an SW41 rotor for 30 min at 4 °C. The membrane band was harvested using a peristaltic pump and analysed by immunoblotting as described above.

Dry cell weight determination. Cell density was measured with a spectrophotometer (model 7315 by Jenway) at a wavelength of 730 nm. The relationship between $OD_{730\ nm}$ and dry cell weight was determined from a 140 ml culture grown under standard conditions to $OD_{730\ nm}$ of 0.716. Three 40 ml samples were taken from this culture for dry cell weight determination. Cells were harvested by centrifugation for 10 min at 3,500 *g* at RT. The supernatant was removed and the cells were washed with 1 ml of PBS. The cell suspension was transferred to pre-weighed 1.5 ml tubes and centrifuged again for 5 min at 3,500 *g* at RT. The supernatant was aspirated and the cell pellets were dried at 80 °C for 24 h and were weighed after cooling in a desiccator. The amount of cells in a litre at one absorbance unit at 730 nm corresponds to 0.258 g_{dcw}.

Chlorophyll-*a* measurement. One millilitre of a cell suspension at an absorbance of 1 at $OD_{730\ nm}$ was pelleted by centrifugation at 3,500 *g* for 10 min at RT. Cells were re-suspended in 100 µl of H_2O then incubated in 900 µl of acetone overnight at 4 °C in the dark. The

extract was centrifuged at 17,000 *g* for 5 min at RT to pellet debris, the supernatant was removed and fluorescence was then measured according to Welschmeyer et al (1994).[34]

Supplementary figure 1. Quantification of CYP1A1. (a) Immunoblot with 30 µg of total protein from Sy21 in triplicate and the BAP-FLAG standard at different concentrations. (b) Plot of BAP-FLAG signal from panel A to generate standard curve for CYP1A1 quantification. The concentration of CYP1A1 was determined to be 6.2 pmol mg^{-1} total protein.

Supplementary figure 2. The inhibitor α-naphthoflavone abolishes CYP1A1 activity. CYP1A1 activity was measured via an EROD (ethoxyresorufin O-deethylation) assay in live cells using a microplate reader. Measurements were made on three biological replicates 1 h after the addition of 5 µM of the substrate ethoxyresorufin. The experiment was repeated three times and results from a typical experiment are shown. Error bars represent the standard error of triplicate measurements. Statistical significances were inferred by the Student's *t* test; ***$P < 0.001$. Addition of 10 µM α-naphthoflavone reduced EROD by 92.9%.

Figure 1

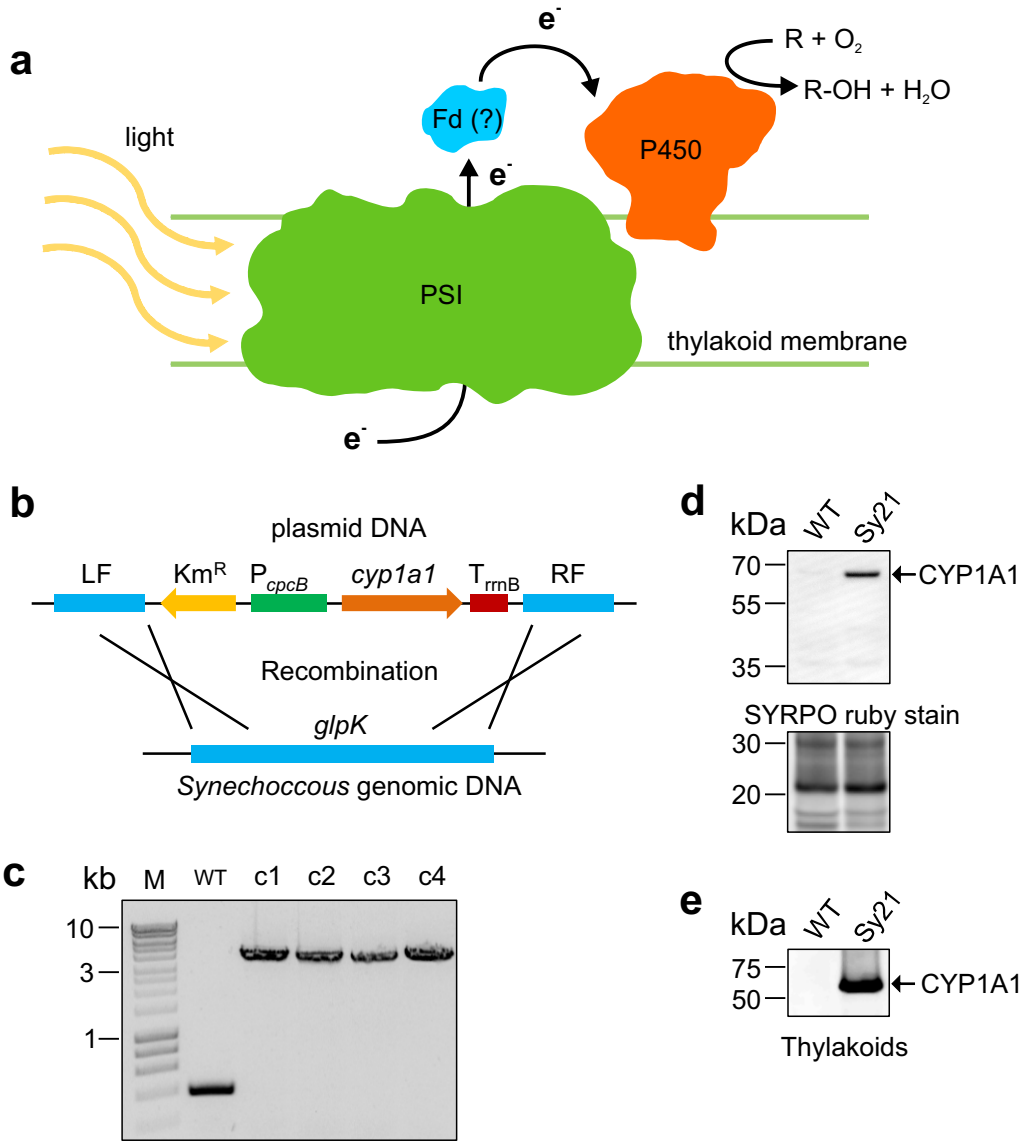
a
e-
R + O2
R-OH + H2O
Fd (?)
P450
light
e-
PSI
thylakoid membrane
e-
b
plasmid DNA
LF
KmR
PcpcB
cyp1a1
TrrnB
RF
Recombination
glpK
Synechoccous genomic DNA
c
kb
M
WT
c1
c2
c3
c4
10
3
1
d
kDa
WT
Sy21
70
55
35
CYP1A1
SYRPO ruby stain
30
20
e
kDa
WT
Sy21
75
50
CYP1A1
Thylakoids

Figure 2

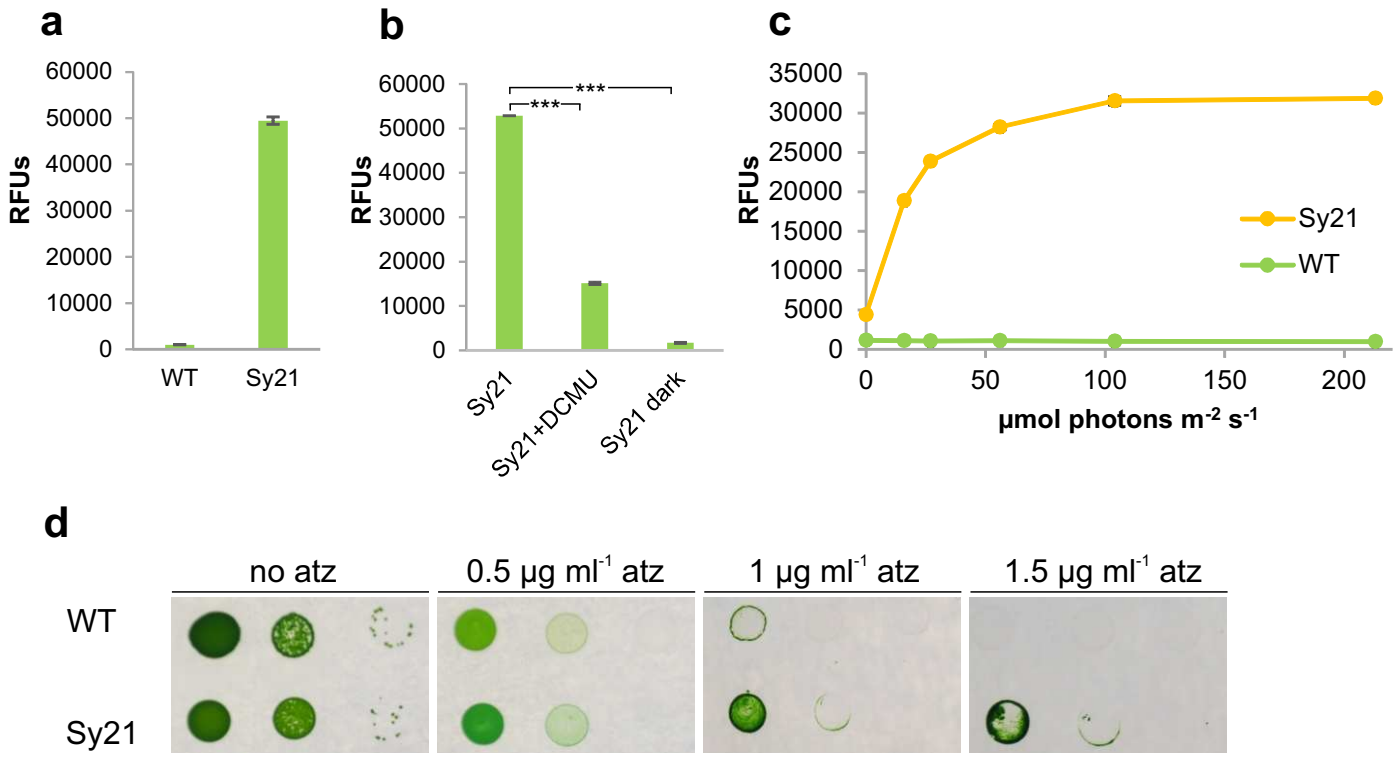
a
RFUs
60000
50000
40000
30000
20000
10000
0
WT
Sy21
b
RFUs
60000
50000
40000
30000
20000
10000
0
***
***
Sy21
Sy21+DCMU
Sy21 dark
c
RFUs
35000
30000
25000
20000
15000
10000
5000
0
0
50
100
150
200
µmol photons m-2 s-1
Sy21
WT

d
no atz
0.5 µg ml-1 atz
1 µg ml-1 atz
1.5 µg ml-1 atz
WT
Sy21

Figure 3

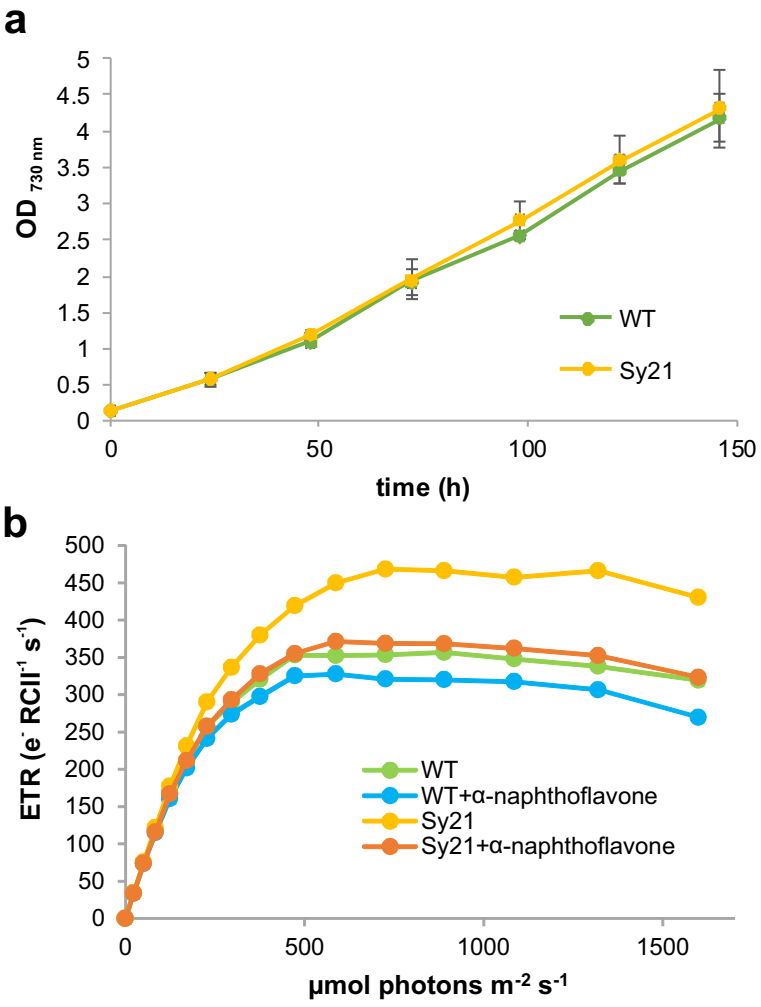
a
OD 730 nm
time (h)
WT
Sy21
b
ETR (e⁻ RCII⁻¹ s⁻¹)
μmol photons m⁻² s⁻¹
WT
WT+α-naphthoflavone
Sy21
Sy21+α-naphthoflavone

Supplementary Figure 1

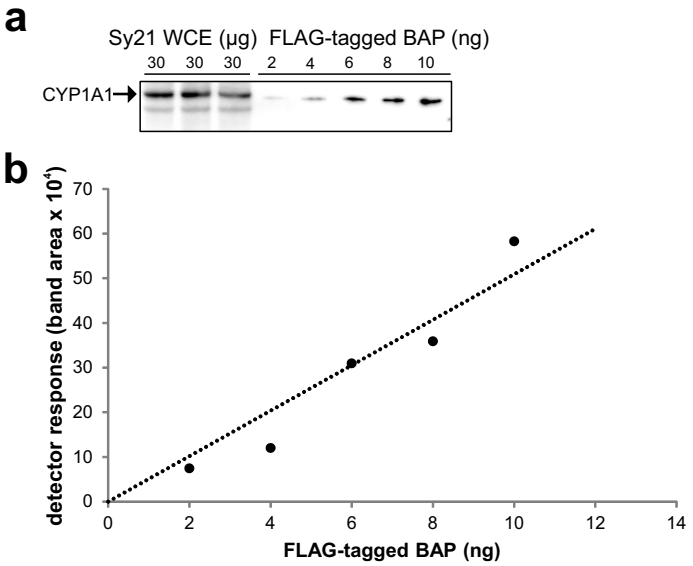

Supplementary Figure 2